Conformational Flexibility of Phosphate, Phosphonate, and Phosphorothioate Methyl Esters in Aqueous Solution

Jan Florián,*,† Marek Štrajbl,‡ and Arieh Warshel†

Contribution from the Department of Chemistry, University of Southern California, Los Angeles, California 90089-1062, and Institute of Physics, Charles University, Ke Karlovu 5, 12116 Prague 2, Czech Republic

Received April 4, 1997. Revised Manuscript Received June 15, 1998

Abstract: The intrinsic rotational barriers of the α and ζ coordinates of the native and modified DNA linkages were examined using neutral and ionic methyl phosphates, phosphorothioates, and phosphonates as model systems. Free energy profiles of the pathways from the right- (g^-g^-) to the left-handed (gg) conformers of dimethyl phosphate anion ($CH_3OP(O_2)OCH_3^-$), dimethyl phosphorothioate anion ($CH_3OP(O)(S)OCH_3^-$), dimethyl methylphosphonate ($CH_3OP(O)(CH_3)OCH_3$), and methyl ethylphosphonate anion ($CH_3CH_2P(O_2)$-OCH_3) were evaluated using ab initio MP2/6-31G+G**//HF/6-31G* quantum mechanical calculations coupled with the Langevin dipoles and polarized continuum solvation models. Differences in the gas-phase conformational properties of the studied molecules were found to diminish in aqueous solution. In solution, the gg (g^-g^-) conformations are the most stable for dimethyl phosphate anion and the neutral phosphonate, whereas the gt conformation was predicted to prevail for dimethyl phosphorothioate anion. For methyl ethylphosphonate anion, which was found to be the most flexible of all the studied molecules, three stable conformations involving the gg, gt^-, and t^-g rotamers were predicted. The calculated activation free energies for the $g^-g^- \leftrightarrow$ gg transition in aqueous solution amount to 2.7, 1.7, 2.1, and 1.5 kcal/mol for the dimethyl phosphate anion, dimethyl phosphorothioate anion, and the neutral and ionic phosphonate ester, respectively. For the S_p and R_p stereoisomers of the DNA linkage containing the neutral phosphonate, the structures of the corresponding transition states involve the cis conformation around the PO_3' or PO_5' bonds, respectively. The calculated similarities in the conformational behavior of the phosphate, phosphorothioate, and phosphonate methyl esters are quite informative. In particular, they provide formal justification for the use of the substitution experiments to study the role of intermolecular interactions involving ionic and ester phosphate oxygens in the stabilization of the structure of nucleic acids and DNA−protein complexes.

1. Introduction

The large flexibility of nucleic acids plays a significant role in the regulation of genetic expression. This flexibility is related to many torsional degrees of freedom around single bonds in the sugar−phosphate backbone. The free energy profile along any of these internal rotations is the result of a complicated interplay between the intrinsic rigidity of chemical bonds, solvation effects, and other intra- and intermolecular interactions. Because the knowledge of the relative importance of these contributions is needed for a better understanding of the function of nucleic acids, numerous experimental and theoretical studies were devoted to this topic. Among them, the crystallographic studies of the right- and left-handed forms of DNA have revealed that the stabilization of a particular DNA conformation is greatly aided by the interactions involving ester and anionic oxygens of phosphate groups.[1−3] The significance of these interactions for the thermodynamics and kinetics of the B-DNA to Z-DNA conformational transition in solution was explored using the stereospecific replacement of the phosphate groups by their phosphorothioate or methylphosphonate analogues.[4−8] In a conceptually similar study, Strauss and Maher[9] demonstrated that DNA bends in the regions containing neutral methylphosphonate linkages. The observed DNA bending was interpreted by these authors as an evidence for the important role of the phosphate−phosphate repulsion for determining the DNA structure and, more generally, as a support for the electrostatic mechanism of DNA bending by sequence-specific DNA binding proteins.[10]

Conclusions of these and related experimental studies rely largely on the assumption that the conformational barriers and equilibria of methylphosphate esters in aqueous solution are not influenced significantly by the replacement of the phosphate oxygens by the $-CH_2-$, $-CH_3$, or $-S$ groups. The validity of this assumption is intuitively not obvious since the anomeric

* Corresponding author. E-mail: florian@usc.edu.
† University of Southern California.
‡ Charles University.

(1) Dickerson, R. E.; Drew, H. R. *J. Mol. Biol.* **1981**, *149*, 761.
(2) Dickerson, R. E. *Methods Enzymol.* **1992**, *211*, 67.
(3) Gessner, R. V.; Frederick, C. A.; Quigley, G. J.; Rich, A.; Wang, A. H. J. *J. Biol. Chem.* **1989**, *264*, 7921.
(4) Callahan, L.; Han, F.-S.; Watt, W.; Duchamp, D.; Kezdy, J. F.; Agarwal, K. *Proc. Natl. Acad. Sci. U.S.A.* **1986**, *83*, 1617.
(5) Jovin, T. M.; McIntosh, L. P.; Arndt-Jovin, D. J.; Zarling, D. A.; Robert-Nicoud, M.; van de Sande, J. H.; Jorgenson, K. F.; Eckstein, F. *J. Biomol. Struct. Dyn.* **1983**, *1*, 21.
(6) Cosstick, R.; Eckstein, F. *Biochemistry* **1985**, *24*, 3630.
(7) Cosstick, R.; Cruse, W. B. T.; Eckstein, F.; Kennard, O.; Salisbury, S. A. *Phosphorus Sulfur Relat. Elem.* **1987**, *30*, 555.
(8) Jovin, T. M.; McIntosh, L. P.; Soumpasis, D. M. *Ann. Rev. Phys. Chem.* **1987**, *38*, 521.
(9) Strauss, J. K.; Maher, L. J., III. *Science* **1994**, *266*, 1829.
(10) Manning, G.; Ebralidse, K. K.; Mirzabekov, A. D.; Rich, A. J. *Biomol. Struct. Dyn.* **1989**, *6*, 877.

S0002-7863(97)01082-2 CCC: $15.00
Published on Web 07/28/1998

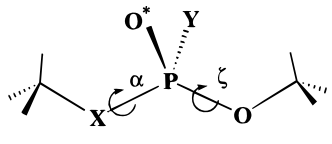

	X	Y
DMP⁻:	O	O
MEPn⁻:	CH_2	O
DMPn:	O	CH_3
DMPTh⁻:	O	S

Figure 1. Structure of DMP^-, MEPn, DMPn, and $DMPTh^-$. In DNA, angles α and ζ correspond to the torsional angles around O5′—P and P—O3′ bonds, respectively. For the purpose of the definition of the *R* and *S* stereoisomers, we assume that the O_5'(X), P, and O_3' atoms lie in the plane of the paper. Then, following the IUPAC convention, the phosphonate methyl ($Y = CH_3$) is directed above and below this plane in the S_p (pseudoaxial) and R_p (pseudoequatorial) stereoisomers of DMPn, respectively, and the sulfur atom ($Y = S$) is directed above and below the plane of the paper in the R_p (pseudoaxial) and S_p (pseudoequatorial) stereoisomers of $DMPTh^-$, respectively.

effects determining gas-phase behavior are generally sensitive to the electronic structure.[11] Furthermore, detailed analysis of the relationship between substitutions in the nucleic acid backbone and its local conformational properties is of significant importance for the rational design of antisense oligonucleotides.[12−18] Finally, the structures of the phosphonate and phosphorothioate esters are important for investigation of enzyme mechanisms,[19−21] the design of catalytic antibodies,[22] and the deactivation of the toxic gas sarin.[23,24]

Considering the importance of the above problems, we carried out ab initio quantum mechanical calculations of the rotational barriers and conformational equilibria in dimethyl phosphate anion (DMP^-), methyl ethylphosphonate anion ($MEPn^-$), dimethyl methylphosphonate (DMPn), and dimethyl phosphorothioate anion ($DMPTh^-$) (Figure 1). In this way, the substituent effects upon the local conformational flexibility of the DNA backbone could be determined. The hydration effects were taken into account using polarized continuum (PCM)[25] and Langevin dipoles (LD)[26−28] solvation models. These calculations represent the first quantum mechanical evaluation of the thermodynamic properties and activation barriers for conformational transitions of phosphate, phosphorothioate, and phosphonate esters in aqueous solution. Previously, gas-phase ab initio calculations of DMP^- (see, for example, refs 29−33 and references therein), DMPn,[34] $DMPTh^-$,[16,35] and methoxy methylphosphonate[36] have been reported.

2. Methods

The (α, ζ) sections of the gas-phase potential energy surfaces (PESs) of DMP^-, DMPn, and $MEPn^-$ were mapped by partial geometry optimizations, in which the torsional angles α and ζ (Figure 1) were kept constant and other degrees of freedom were relaxed. In these calculations, angles α and ζ were varied in 60° increments. This sketch of the PES was further refined in the low-energy regions by additional partial geometry optimizations. The minima and transition state (TS) geometries were calculated by full geometry optimizations started from the structures selected on the basis of this PES and molecular symmetry. The search for the stationary points of $DMPTh^-$ was initiated from the (α, ζ) values calculated previously for DMP^-. These partial and full geometry optimizations were carried out at the ab initio HF/6-31G* level of theory. The character of the calculated stationary points and zero-point vibrational energies (ZPEs) were evaluated by subsequent calculations of the HF/6-31G* harmonic vibrational frequencies. The effects of electron correlation on the relative stabilities of the stationary points were examined by using the second-order Møller−Plesset perturbation theory (MP2) and the 6-31+G** basis set, which contained diffuse and polarization functions. These MP2 calculations were carried out for the HF/6-31G*-optimized geometries. In addition, the MP2 method with a smaller (6-31G**) basis set was used to reoptimize geometries of the gauche−gauche (gg)[37] conformers. The ab initio calculations were carried out with the Gaussian 94 program.[38]

Solvation free energies were calculated by using the LD solvation model.[28,39−41] This model evaluates an average polarization of the solvent molecules surrounding the solute using the discrete dipolar representation, which was parametrized to reproduce experimental solvation free energies (ΔG_{solv}) of a representative set of small neutral

(11) *The anomeric effects and associated stereoelectronic effects*; Thatcher, G. R. J., Ed.; American Chemical Society: Washington, DC, 1993; Vol. 539.
(12) Miller, P. S.; McParland, K. B.; Jayaraman, K.; Ts'O, P. O. P. *Biochemistry* **1981**, *20*, 1874.
(13) Sarin, P. S.; Agrawal, S.; Civeira, M. P.; Goodchild, J.; Ikeuchi, T.; Zamecnik, P. C. *Proc. Natl. Acad. Sci. U.S.A.* **1988**, *85*, 7448.
(14) Eckstein, F.; Gish, G. *Trends Biochem. Sci.* **1989**, *14*, 97−100.
(15) Miller, P. S.; Bhan, P.; Cushman, C. D.; Kean, J. M.; Levis, J. T. *Nucleosides Nucleotides* **1991**, *10*, 37.
(16) Jaroszewski, J. W.; Syi, J. L.; Maizel, J.; Cohen, J. S. *Anti-Cancer Drug Des.* **1992**, *7*, 253.
(17) De Mesmaeker, A.; Haner, R.; Martin, P.; Moser, H. E. *Acc. Chem. Res.* **1995**, *28*, 366.
(18) Haly, B.; Bellon, L.; Mohan, V.; Sanghvi, Y. *Nucleosides Nucleotides* **1996**, *15*, 1383.
(19) Eckstein, F. *Angew. Chem., Int. Ed. Engl.* **1975**, *14*, 160.
(20) Kurpiewski, M. R.; Koziolkiewicz, M.; Wilk, A.; Stec, J. W.; Jenjacobson, L. *Biochemistry* **1996**, *35*, 8846.
(21) Thorogood, H.; Grasby, J. A.; Connolly, B. A. *J. Biol. Chem.* **1996**, *271*, 8855.
(22) Tramontano, A.; Janda, K. D.; Lerner, R. A. *Science* **1986**, *234*, 1566.
(23) Henderson, M. A.; White, J. M. *J. Am. Chem. Soc.* **1988**, *110*, 6939.
(24) Bertilsson, L.; Potje-Kamloth, K.; Liess, H.-D.; Engquist, I.; Liedberg, B. *J. Phys. Chem. B* **1998**, *102*, 1260.
(25) Tomasi, J.; Mennucci, B.; Cammi, R.; Cossi, M. In *Computational approaches to biochemical reactivity*; Naray-Szabo, G., Warshel, A., Eds.; Kluwer Academic Publishers: Dordrecht, The Netherlands, 1997; p 1.
(26) Warshel, A.; Russell, S. T. *Q. Rev. Biol.* **1984**, *17*, 283.
(27) Lee, F. S.; Chu, Z. T.; Warshel, A. *J. Comput. Chem.* **1993**, *14*, 161.
(28) Florián, J.; Warshel, A. *J. Phys. Chem. B* **1997**, *101*, 5583.
(29) Liang, C.; Ewig, C. S.; Stouch, T. R.; Hagler, A. T. *J. Am. Chem. Soc.* **1993**, *115*, 1537.
(30) Landin, J.; Pascher, I.; Cremer, D. *J. Phys. Chem.* **1995**, *99*, 4471.
(31) Florián, J.; Baumruk, V.; Strajbl, M.; Bednárová, L.; Stepánek, J. *J. Phys. Chem.* **1996**, *100*, 1559.
(32) Schneider, B.; Kabelác, M.; Hobza, P. *J. Am. Chem. Soc.* **1996**, *118*, 12207.
(33) MacKerell, A. D., Jr. *J. Chim. Phys.* **1997**, *94*, 1436.
(34) Hausheer, F. H.; Singh, U. C.; Palmer, T. C.; Saxe, J. D. *J. Am. Chem. Soc.* **1990**, *112*, 9468.
(35) Steinke, C. A.; Reeves, K. K.; Powell, J. W.; Lee, S. A.; Chen, Y. Z.; Wyrzykiewicz, T.; Griffey, R. H.; Mohan, V. *J. Biomol. Struct. Dyn.* **1997**, *14*, 509.
(36) Strajbl, M.; Florián, J. *J. Biomol. Struct. Dyn.* **1996**, *13*, 687.
(37) Two distinct classification systems are common in the field of conformational analysis. As the stable conformers have usually torsional angles near 60°, −60°, and 180°, the corresponding angles are denoted in the notation used mostly in spectroscopy as gauche (g), gauche⁻ (g⁻), and trans (t), respectively. In addition, this notation denotes angles near 0° as cis (c). The alternative system uses notation sp, sc, ac, and ap for the torsional angles near 0, 60, 120, and 180°, respectively. The spectroscopic notation is used throughout this work. For the structures in which torsional angles fall beyond gauche and trans regions the relevant torsional angles will be mentioned explicitly.
(38) Frisch, M. J.; Trucks, G. W.; Schlegel, H. B.; Gill, P. M. W.; Johnson, B. G.; Robb, M. A.; Cheeseman, J. R.; Keith, T.; Petersson, G. A.; Montgomery, J. A.; Raghavachari, K.; Al-Laham, M. A.; Zakrzewski, V. G.; Ortiz, J. V.; Foresman, J. B.; Cioslowski, J.; Stefanov, B. B.; Nanayakkara, A.; Challacombe, M.; Peng, C. Y.; Ayala, P. Y.; Chen, W.; Wong, M. W.; Andres, J. L.; Replogle, E. S.; Gomperts, R.; Martin, R. L.; Fox, D. J.; Binkley, J. S.; Defrees, D. J.; Baker, J.; Stewart, J. P.; Head-Gordon, M.; Gonzalez, C.; Pople, J. A. *Gaussian 94, Revision D.2*; Gaussian, Inc.: Pittsburgh, PA, 1995.
(39) Warshel, A. *J. Phys. Chem.* **1979**, *83*, 1640.
(40) Russell, S. T.; Warshel, A. *J. Mol. Biol.* **1985**, *185*, 389.
(41) Muller, R. P.; Florián, J.; Warshel, A. *NATO ASI* **1997**, *E342*, 47.

and ionic molecules. Here we used the recent ab initio version of the LD model developed for aqueous solutions.[28] This version uses potential-derived HF/6-31G* and MP2/6-31+G** atomic charges to represent the charge distribution of the solute molecules. The conformation-dependent atomic charges of DMP^-, $DMPTh^-$, and DMPn that were used for the calculation of ΔG_{solv} are presented in the Supporting Information (Tables 1S−3S). The contributions to the ΔG_{solv} due to the solute polarization by the solvent (induction effects) were included in the calculated solvation free energies by using solute charges evaluated for a model where the solvent is represented by a continuum dielectric ($\epsilon = 80$). The PCM model[42,43] implemented in the Gaussian 94 program was used to calculate these solvated atomic charges. For the PCM calculations, the default Pauling's atomic radii multiplied by a standard factor of 1.2[44] were used. The ΔG_{solv} calculations were carried out for the gas-phase HF/6-31G* geometries of the stationary points using the program ChemSol.[45]

For the sake of comparison, the electrostatic part of ΔG_{solv} was also evaluated using the PCM in the implementation mentioned above (Tables 1S−3S). Interestingly, the magnitudes of the conformation-dependent variations in the solvation free energy ($\Delta\Delta G_{solv}$) calculated by the LD model turned out to be systematically larger than the corresponding PCM results. A similar trend was obtained previously for ethanediol.[28] The largest differences between the magnitudes of PCM and LD energies were found for DMPn. Here, the LD energies showed a more reasonable dependence on the dipole moment than the PCM energies (see also the section 3.2.3). To assess more thoroughly the performance of these methods for conformational equilibria, we carried out additional calculations for trimethyl phosphate and compared the resulting LD and PCM energies with the available experimental estimates.[46] On the basis of these comparisons and also the facts that the LD energies involve the hydrophobic term and provide more accurate pK_a values of methyl phosphates,[50] we consider the LD $\Delta\Delta G_{solv}$ energies obtained in this study to be superior to the corresponding PCM results.

The relative free energies were determined as differences in standard free energies in aqueous solution (1 M aqueous solution, 1 M gas, 298 K, 1 atm). These free energies were calculated as the sum of the MP2/6-31+G(d,p)//HF/6-31G* gas-phase energy, the HF/6-31G(d) zero-point vibrational energy (ZPE) multiplied by the factor 0.9, the $T\Delta S$ term evaluated using the rigid-rotor approximation,[51] and the hydration free energy (ΔG_{solv}). (Note that the enthalpic and entropic contributions that originate from the solvent degrees of freedom are implicitly included in the calculated ΔG_{solv}.) The harmonic vibrational contributions to the gas-phase enthalpies and entropies at 298 K and contributions of symmetry-related degeneracies were included in the calculated free energy differences between the individual conformers of the title compounds (ΔG).

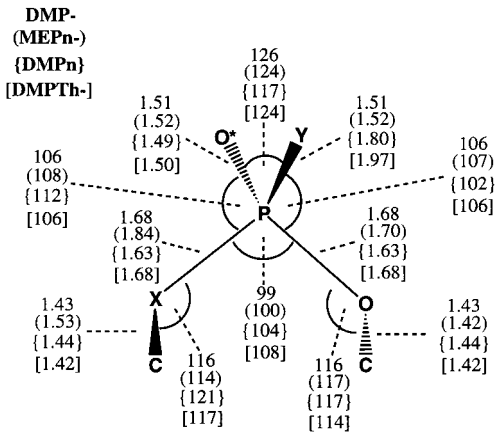

Figure 2. Comparison of the MP2/6-31G** geometry (Å, deg) of the gg conformers of phosphate, phosphonate, and phosphorothioate methyl esters. The (α, ζ) torsional angles calculated at the MP2/6-31G** level are (69.8°, 69.8°), (62.3°, 83.3°), (48.1°, 82.1°), and (63.0°; 70.9°) for DMP^-, $MEPn^-$, DMPn (S_p), and $DMPTh^-$ (R_p), respectively.

For the sake of comparison of the intrinsic flexibility of different phosphate and phosphonate esters that are embedded in the (nonsymmetric) DNA backbone, the symmetry-related degeneracies of the individual stationary points were excluded from the free energy profiles for the g^-g^- to gg conformational transition (Δg^{DNA}). In addition, vibrational contributions (except for ZPE) to Δg^{DNA} were neglected. This is because the largest part of these contributions can be attributed to the low-frequency normal modes involving α and ζ torsions. However, due to the presence of the dangling methyl groups, the frequencies of these normal modes are significantly underestimated in the model compounds used by us. Consequently, the corresponding vibrational contributions to Δg^{DNA} would be largely overestimated. Moreover, the harmonic oscillator model that is commonly used for the evaluation of the vibrational contributions to the gas-phase enthalpies and entropies at 298 K is not fully valid for highly flexible molecules.[52]

3. Results and Discussion

3.1. Substituent Effects on the Geometry and Charge Localization. The *geometries and atomic charges of the gg conformers*[37] of the studied compounds (Figure 1) are compared in Figure 2 and Table 1. More detailed information, including the stereoelectronic effects on the atomic charges, dipole moments, and the individual components of the solvation free energies, are presented in Figure 1S and Tables 1S−5S of the Supporting Information. Below, we discuss major changes in the charge distribution and bonding that accompany the substitution of the oxygen atoms of the phosphate group by the $-CH_2-$, $-CH_3$, and $-S$ groups.

The excess negative charge of about −0.2 au, which is created by replacing the partially negatively charged methoxy group of DMP^- by the neutral ethyl group, is uniformly distributed in $MEPn^-$ over oxygen and phosphorus atoms. As a result, the PO and PO* bond lengths are slightly longer in $MEPn^-$ than in DMP^-. Also the PC bond is by 0.16 Å longer than the corresponding PO bond, but a small lengthening of the DNA backbone due to the $-CH_2-$ group substitution for the ester

(42) Miertus, S.; Scrocco, E.; Tomasi, J. *Chem. Phys.* **1981**, *55*, 117.
(43) Miertus, S.; Tomasi, J. *Chem. Phys.* **1982**, *65*, 239.
(44) Tomasi, J.; Persico, M. *Chem. Rev.* **1994**, *94*, 2027.
(45) Florián, J.; Warshel, A. *ChemSol, Version 1.0*; University of Southern California, 1997.
(46) Note that there are no experimental data available for the hydration free energy differences between different conformers of ionic molecules and that experiments available for neutral compounds are rather inaccurate. For example, $\Delta\Delta G_{solv}$ (vapor → cyclohexane) = −0.5 kcal/mol for the ggg and tgg conformers of trimethyl phosphate can be determined from the measured relative IR intensities of the P═O stretching bands of these conformers[47] if one assumes that the intensities of these bands are solvent-independent. Unfortunately, the individual components of the P═O stretching band cannot be distinguished in aqueous solution. Using instead the relative intensities of the ggg and tgg components of the PO_3 symmetric stretching band in cyclohexane and water,[47] we calculated $\Delta\Delta G_{solv}$ (cyclohexane → water) = −2.0 kcal/mol. Adding these energies, we arrived to $\Delta\Delta G_{solv}$ (vapor → water) = −2.5 kcal/mol, which agrees well with the corresponding LD result of −2.0 kcal/mol. On the other hand, PCM calculation of the hydration free energy difference between the ggg and tgg conformers of trimethyl phosphate resulted in $\Delta\Delta G_{solv}$ = −0.7 kcal/mol. Also, favorable agreement with the experimentally observed trends was obtained by using the LD model for the tautomeric equilibria of protonated cytosine[48] and the pseudorotational barrier in tetrahydrofuran.[49] Finally, the results obtained with the LD model for different conformers of ethanediol were found to be in a good agreement with the results of all-atom solvent models (see ref 28).
(47) Streck, R.; Barnes, A. J.; Herrebout, W. A.; van der Veken, B. J. *J. Mol. Struct.* **1996**, *376*, 277.
(48) Florián, J.; Baumruk, V.; Leszczynski, J. *J Phys. Chem.* **1996**, *100*, 5578.
(49) Strajbl, M.; Baumruk, V.; Florián, J. *J. Phys. Chem. B* **1998**, *102*, 1314.
(50) Florián, J.; Warshel, A. *J. Phys. Chem.* **1998**, *102*, 719.
(51) McQuarrie, D. A. *Statistical Mechanics*; Harper & Row: New York, 1976.
(52) Herzberg, G. *Infrared and Raman Spectra of Polyatomic Molecules*; Van Nostrand: New York, 1945.

Table 1. Comparison of Atomic Charges[a] of the gg Conformers of Phosphate, Phosphonate, and Phosphorothioate Methyl Esters

atom[b]	DMP^-	$MEPn^-$	DMPn	$DMPTh^-$
P	1.49	1.42	1.31	0.89
O*	−0.92	−0.99	−0.80	−0.82
Y	−0.92	−0.96	−0.10	−0.66
X	−0.58	−0.11	−0.50	−0.44
Cl	0.26	0.01	0.28	0.25
O	−0.58	−0.59	−0.46	−0.51
C2	0.26	0.24	0.27	0.29

[a] The atomic charges (au) were obtained by fitting to the PCM HF/6-31G* electrostatic potential. [b] For atom notation see Figure 1. Symbols C1 and C2 denote carbon atoms bonded to X and O, respectively. The charges presented for the carbon atoms correspond to the total charge of the corresponding methylene or methyl groups. The estimated fit uncertainties (au) are 0.06, 0.03, 0.02, 0.01, and 0.01 for P, C, S, O, and O*, respectively.

oxygen is not expected to perturb DNA structure significantly. In fact, even extended DNA linkages containing an *inserted* methylene group were shown to be compatible with duplex DNA structures.[18,36]

An obvious consequence of the replacement of one of the ionic oxygens of DMP^- by the methyl group is the change in the total charge from −1 to 0. A large portion (0.82 au) of this change can be recovered as the difference in charges of −O* and $-CH_3$ groups in DMP^- and DMPn, whereas the remaining part of the overall charge difference is accomodated by the oxygen atoms of DMPn that are less negatively charged than their DMP^- counterparts (Table 1). These charge variations are accompanied with shortening of the PO* and PO bonds (Figure 2). However, the calculated change of 0.02 Å in the PO* bond length is quite small and does not support the presence of a P═O* double bond in DMPn. Similarly, neither P═O* nor P═S bonding is consistent with the calculated geometry of $DMPTh^-$. For example, the calculated difference in the PO* bond lengths of gg conformers of DMP^- and $DMPTh^-$ is smaller than 0.01 Å. As far as the charge distribution is concerned, the negative charge was calculated to be delocalized over both the O* and S atoms in $DMPTh^-$, supporting thus the resonance structure **1**, wherein the PO* and PS bond orders are

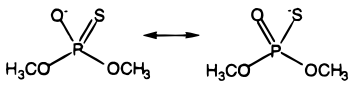

1

close to 1.5. Interestingly, the issue of the PO* and PS bond orders in phosphorothioate diesters has often been disputed. In particular, it has been shown that the crystallographic data support the left-side structure in **1** as a dominant structural form of $DMPTh^-$.[53] On the other hand, the NMR and pK_a data were interpreted as an evidence that the PO* bond order approaches 2 in *O,O*-dialkyl phosphorothioates.[54]

3.2. Free Energy Profiles for the Conformational Transitions of the Modified Phosphodiester Linkages. The conformational *transition from the right- to the left-handed DNA* structure involves rotations around P—O5′ (α) and P—O3′ (ζ) bonds of the phosphodiester linkage (Figure 1). These torsional angles usually adopt g^-g^- values[37] for right-handed DNA structures,[1,55] whereas in Z-DNA, the gg and tg conformations prevail.[3,55] Thus, we have chosen the g^-g^- to gg transition as

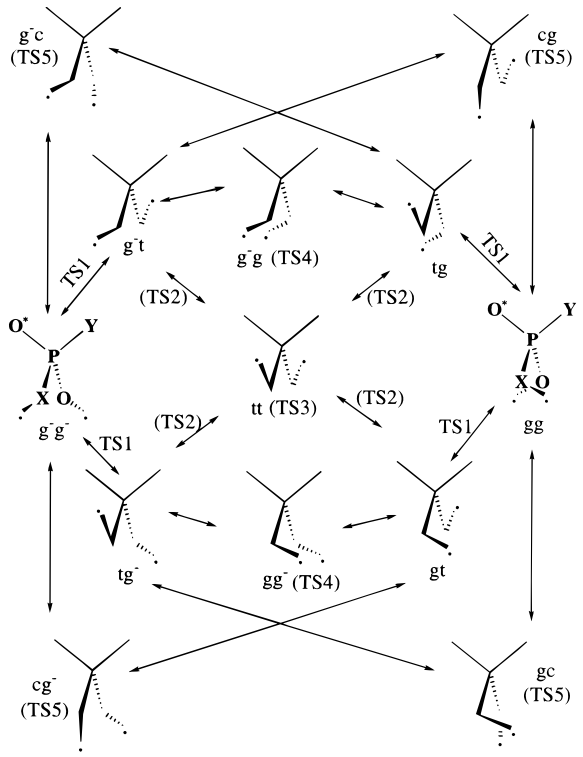

Figure 3. Schematic representation of the possible interconversion pathways between the g^-g^- and gg conformers of phosphate and phosphonate esters.

the most natural and informative benchmark for the comparison of the local conformational flexibility of modified phosphodiester linkages.[56] The general mechanisms available for this transition are depicted in Figure 3, whereas the calculated relative energies of individual stationary points in gas phase and aqueous solution are presented in Figure 4 and Table 2.

3.2.1. Dimethyl Phosphate Anion (DMP^-). The gg conformer corresponds to a global minimum on the free energy surface of DMP^- (Table 2) in both gas phase and solution. Although the magnitudes of the dipole moment vary significantly among various conformers (Table 1S), the conformation dependence of the solvation free energy (ΔG_{solv}) is rather small. This is because the orientations of the solvent dipoles around a small molecular ion are largely determined by its charge. If the dipole moment of a negatively charged solute increases, the increase in the solute−solvent interactions on a more negative side of the solute is compensated by the decrease of these interactions on the opposite side. However, if the dipole moment of such anion exceeds a certain critical size that allows the solute dipoles on its positive end to reorient, this compensating effect disappears and a further increase in the dipole moment leads to a larger solvation stabilization. The highest barrier for the *g^-g^- ↔ gg transition in DMP^-* is determined by the relative free energy of the TS1 transition structure, which amounts to

(53) Schwalbe, C. H.; Goody, R.; Saenger, W. *Acta Crystallogr.* **1973**, *B29*, 2264.
(54) Frey, P. A.; Sammons, R. D. *Science* **1985**, *228*, 541.
(55) Schneider, B.; Neidle, S.; Berman, H. M. *Biopolymers* **1997**, *42*, 113.

(56) The gg and g^-g^- conformers of DMP^- are symmetrically equivalent, but they correspond to the separate left- and right-handed conformers when they are inserted in DNA or RNA. In such a case, gg and g^-g^- conformers are not exactly isoenergetic. Yet, the free energy barriers of phosphoester bonds contribute to the overall kinetics of the DNA and RNA conformational transitions. We assume that these intrinsic barriers can be reasonably modeled by rotational barriers of DMP^- in aqueous solution. Naturally, the intrinsic flexibility of the α and ζ coordinates derived from the conformational properties of DMP^- do not include the coupling with other torsional coordinates of the DNA backbone and sequence-dependent effects. However, this deficiency of our model is of less importance for the evaluation of the local conformational effects of the chemical modifications of the phosphate group that are the main theme of the present work.

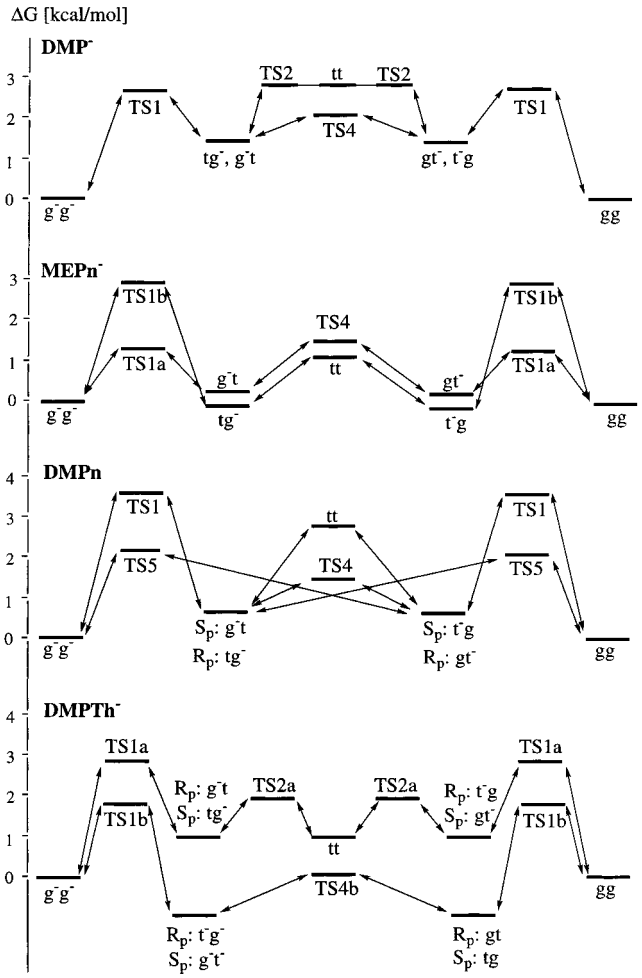

Figure 4. Calculated free energy profiles (Δg_{DNA}) along the low-energy reaction coordinates for the g^-g^- to gg conformational transition in phosphate, phosphonate, and phosphorothioate methyl esters.

2.0 kcal/mol in the gas phase, and increases to 2.7 kcal/mol upon solvation. From the g^-t or tg^- conformer, the lowest energy pathway proceeds via the g^-g or gg^- transition structures denoted as TS4. This stationary point is notably stabilized by hydration. This stabilization was found to be mostly due to the electrostatic part of the ΔG_{solv} (Table 4S), which is consistent with very large dipole moment of this conformer (Table 1S). The alternative pathway proceeding via TS2 and TS3 transition states was calculated to have a higher barrier. However, this result should be taken with caution since the involved free energy differences are close to the error range of our method, and the PCM calculations indicate that the second pathway is energetically more feasible. The overall free energy barrier for the $g^-g^- \leftrightarrow$ gg transition is predicted to be near 2.7 kcal/mol by both the LD and PCM solvation models.

Depending on the order in which the α and ζ coordinates vary between the g^- and g regions, there are two different pathways of the same energy that connect the g^-g^- and gg conformations of DMP^-. The substitution of the ionic or ester oxygen removes this degeneracy. In addition, pathways involving cis or tt conformers become more favorable in phosphonate esters (see below).

3.2.2. Methyl Ethylphosphonate Anion ($MEPn^-$). For $MEPn^-$, we assume that the methylene group replaces the O5′ oxygen (Figure 1). The generalization to the case of the methylene substitution in the O3′ position can be made by simply exchanging values of the α and ζ angles. The calculated free energies of the gg, gt^-, and t^-g rotamers of $MEPn^-$ are very similar in both solution and gas phase (Table 1). The transitions between these low-energy rotamers and also between the g^-g^- and gg conformers have very low barriers of about 1.5 kcal/mol. These features indicate that $MEPn^-$ is the least rigid of all the systems studied in this work. Interestingly, the increased flexibility of the phosphono ester linkage was suggested more than 20 years ago[57] as an explanation for the observed decrease in the nucleobase stacking in U*pc*A (*pc* indicates 3′-methylene phosphonate linkage) compared to the U*p*A control. However, the subtle differences in the conformational energy profiles of the ionic phosphate and phosphonate linkages become less important for the secondary structures of longer oligonucleotides.[58,59]

3.2.3. Dimethyl Methylphosphonate (DMPn). Because of the replacement of one anionic oxygen by the methyl group, the torsional angles α and ζ are not equivalent in the gg conformer of DMPn. Moreover, upon inserting the DMPn unit in the DNA structure, the phosphorus atom becomes chiral. For the S_p stereoisomer defined in Figure 1, the gg conformer has the torsional angles α and ζ equal to 47.5° and 88.9°, whereas in the g^-g^- conformer, these angles amount to −88.9° and −47.5°, respectively. The gg (g^-g^-) conformation represents the global minimum in aqueous solution, but the energy gap between these and the t^-g and g^-g conformers is smaller than in DMP^-. Moreover, the g^-g conformations span a very wide isoenergetic region ranging from (−123°, 78.5°) to (−78°, 123°). In fact, even the t^-g (−151°, 75°) and g^-t (−75°, 151°) conformers can be considered to be a part of this configuration region.

The conformational stability of DMPn is strongly affected by aqueous solvation. In particular, the gas-phase calculations favor the t^-g and g^-g conformers over the gg (g^-g^-) conformer. The gas-phase stability of the t^-g and g^-g conformers is related to the decreased electrostatic repulsion due to the larger distances between methyl groups. In solution, the long-range electrostatic effects are screened by solvent polarization. In addition, hydrophobic effects tend to prefer conformations with more closely spaced methyl groups, such as in gg and g^-g^- conformers. Indeed the hydrophobic part accounts for as much as 40% of the total ΔG_{solv} difference between the gg and t^-g conformers. The remaining part of this difference involves the electrostatic terms (Table 4S). Here, both the iterative (ILD) and noniterative (NLD) implementations of the LD model predict systematically larger differences between different conformers of DMPn than the PCM method (Table 2S). A similar trend was observed in our previous study of the ethanediol, where the PCM model provided smaller conformation-dependent changes in ΔG_{solv} than the LD model or the all-atom solvent models.[28] In the absence of the relevant experimental data, the LD results seem to be more consistent with the large changes of the dipole moment of DMPn (Table 3S), since the solvation free energy of the neutral solute is expected to be approximately proportional to the square of the solute dipole moment.[60] Moreover, the stabilization of gg conformations in aqueous solution is consistent with the observed conformation of DMPn (R_p) in the d(Cp(CH_3)G) dinucleotide.[61] In this crystal, two symmetrically

(57) Johnson, N. P.; Schleich, T. *Biochemistry* **1974**, *13*, 981.
(58) Breaker, R. R.; Gough, G. R.; Gilham, P. T. *Biochemistry* **1993**, *32*, 9125.
(59) Heinemann, U.; Rudolph, L.-N.; Alings, C.; Morr, M.; Heikens, W.; Frank, R.; Blocker, H. *Nucleic Acids Res.* **1991**, *19*, 427.
(60) Onsager, L. *J. Am. Chem. Soc.* **1938**, *58*, 1486.
(61) Han, F.; Watt, W.; Duchamp, J. D.; Callahan, L.; Kezdy, F. J.; Agarwal, K. *Nucleic Acids Res.* **1990**, *18*, 2759.

Table 2. Relative Stabilities (kcal/mol) of Various Conformers of Phosphate, Phosphonate, and Phosphorothioate Methyl Esters in Gas Phase and Aqueous Solution

conformer (α, ζ)[a]	$\Delta H_{gas}{}^{0}$ [b]	$\Delta H_{gas}{}^{298}$ [b]	$-T\Delta S_{gas}$ [c]	$\Delta\Delta G_{solv}$ [d]	ΔG [e]	Δg_{DNA} [f]
			DMP^-			
gg (75.1, 75.1)	0.0	0.0	0.0	0.0	0.0	0.0
TS1 (136.4, 74.2)	2.0	1.6	0.9	0.7	3.2	2.7
t⁻g (−170.4, 73.8)	1.3	1.4	−0.6	0.2	1.0	1.5
TS2 (160.2, 145.9)	3.2	2.9	0.4	−0.4	2.9	2.8
tt (155.6, 155.6)	3.2	3.5	−1.8	−0.4	1.3	2.8
TS3 (180, 180)	3.6	3.4	0.2	−0.5	3.5	3.1
TS4 (−94.8, 94.8)	2.9	2.5	0.6	−1.0	2.1	1.9
TS5 (−1.9, 112.4)	6.6	6.3	0.7	−0.5	6.5	6.1
			$MEPn^-$			
gg (64.3, 90.8)	0.0	0.0	0.0	0.0	0.0	0.0
TS1a (63.5, 120.5)	0.6	0.1	1.1	0.6	1.8	1.2
gt⁻ (65.8, −171.5)	−0.1	−0.1	−0.5	0.3	−0.3	0.2
TS1b (120.8, 86.4)	3.2	2.7	1.2	−0.3	3.6	2.9
t⁻g (−179.6, 93.4)	0.6	0.6	−0.2	−0.7	−0.3	−0.1
TS2a (121.4, −178.7)	2.6	2.1	0.8	0.2	3.1	3.1
TS2b (179.2, 118.5)	1.0	0.5	1.0	−0.1	1.4	0.9
tt (180, 180)	0.5	0.5	−0.7	0.5	0.7	1.0
TS4 (−119.9, 85.7)	3.1	2.6	1.2	−1.3	2.2	1.5
TS5 (81.8, −3.8)	8.6	8.1	1.1	−2.8	6.4	5.8
TS6 (0.0, 180.0)	3.9	3.4	0.7	0.5	5.1	4.4
			DMPn[g]			
gg (47.5, 88.9)	0.0	0.0	0.0	0.0	0.0	0.0
TS1 (113.4, 80.7)	3.3	2.8	0.9	0.4	4.1	3.7
t⁻g (−151.0, 74.9)	−2.3	−2.3	−0.2	3.0	0.5	0.7
TS3 (−123.9, 78.5)	−2.0	−2.5	0.9	3.1	1.5	1.1
g⁻g (−87.3, 110.1)	−2.1	−2.0	−1.1	3.4	0.3	1.3
TS4 (−98.5, 98.5)	−2.1	−2.6	1.0	3.4	2.2	1.3
TS5 (1.5, 110.2)	1.3	0.8	0.9	0.8	2.5	2.1
gg⁻ (98.5, −98.5)[h]	10.2	9.2	2.8	−4.0	8.4	6.2
tt (180.0, 180.0)[i]	3.1	2.2	1.7	−0.3	4.0	2.8
tg (180.0, 74.0)[h]	3.2	3.2	0.0	−0.1	3.1	3.1
			$DMPTh^{-}$[g]			
gg (64.9, 77.3)	0.0	0.0	0.0	0.0	0.0	0.0
TS1a (124.2, 74.3)	2.4	2.0	0.9	0.4	3.3	2.8
t⁻g (−169.2, 73.7)	0.3	0.3	−0.3	0.7	0.7	1.0
TS1b (61.7, 120.7)	1.3	0.8	1.0	0.4	2.2	1.7
gt (62.1, 172.9)	−0.3	−0.2	−0.3	−0.7	−1.2	−1.0
TS2a (−175.8, 125.3)	2.2	1.7	0.8	−0.3	2.2	1.9
TS2b (124.5, 166.0)	2.2	1.7	0.9	−0.4	2.2	1.8
tt (−171.8, 171.8)	1.3	1.4	−0.5	−0.3	0.6	1.0
TS4a (−98.6, 98.6)	3.3	2.9	0.5	−0.4	3.4	2.9
TS4b (86.3, −86.3)	3.1	2.8	0.4	−2.9	0.7	0.2
TS5 (−4.5, 170.3)	4.2	3.7	1.0	0.0	4.7	4.2

[a] Classification and torsional angles (deg) of the stationary points are based on the gas-phase potential energy surface. Transition states are denoted by the letters TS. If not indicated otherwise, other structures correspond to the minima. Only structurally unique conformers are listed. Torsional angles of symmetrically equivalent conformers can be generated as follows: (α, ζ) = (−ζ, −α) = (−α, −ζ) = (ζ, α) for DMP^-, (α, ζ) = (−ζ, −α) for each stereoisomer of DMPn and $DMPTh^-$, and (α, ζ) = (−α, −ζ) for $MEPn^-$. Torsional angles have positive values if the more distant bond, viewed in the direction along the central bond, is rotated clockwise from the eclipsed (cis) arrangement. [b] Symbols $\Delta H_{gas}{}^{0}$ and $\Delta H_{gas}{}^{298}$ denote the relative gas-phase enthalpies at 0 and 298 K, respectively. $\Delta H_{gas}{}^{0} = \Delta E_{gas} + \Delta ZPE$. The total MP2/6-31+G**//HF/6-31G* energies (E_{gas}) of reference structures amount to −720.702 379, −684.824 637, −685.345 887, and −1043.284 281 au, for the gg conformers of DMP^-, $MePn^-$, DMPn, and $DMPTh^-$, respectively. [c] Relative gas-phase entropies, ΔS_{gas}, were calculated as a sum of the rotational and vibrational contributions. Since the rotational contributions to ΔS_{gas} fall below 0.1 kcal/mol, the presented $T\Delta S$ values correspond effectively to $T\Delta S_{vib}$. [d] Relative solvation free energy calculated by using the MP2-ILD method.[28] The following van der Waals atomic radii were used for the LD calculation: P, 3.1 Å; S, 3.2 Å; C, 2.5 Å; O*, 2.8 Å; O(ester), 2.35 Å; H, 2.2 Å. The absolute MP2-ILD solvation free energies (averaged over 50 randomly chosen origins of the cubic dipole grid) amount to −72.4, −70.3, −10.4, and −68.4 kcal/mol for the gg conformers of DMP^-, $MePn^-$, DMPn, and $DMPTh^-$, respectively. [e] The total free energy differences, $\Delta G = \Delta H_{gas}{}^{298} - T\Delta S_{gas} - RT \ln \omega + \Delta\Delta G_{solv}$. We estimate the uncertainty of ΔG_{total} (and Δg^{DNA}) to be 0.7 kcal/mol. The largest part of this uncertainty can be attributed to the $\Delta\Delta G_{solv}$ term. [f] Intrinsic contributions of the phosphate, phosphorothioate, and phosphonate linkages to the potential of the mean force for the B-to-Z DNA conformational transition, $\Delta g_{DNA} = \Delta H_{gas}{}^{0} + \Delta\Delta G_{solv}$. [g] The (α, ζ) values presented in this table correspond to the S_p stereoisomers of DMPn and R_p stereoisomers of $DMPTh^-$. (Note that, although isolated DMPn and $DMPTh^-$ molecules are achiral, stereocenters appear when these molecules are considered as a part of the DNA backbone in the orientation defined in Figure 1.) The isoenergetic stationary points for the R_p stereoisomer of DMPn (S_p stereoisomer of $DMPTh^-$) can be generated as mirror images with the reflection plane defined by the X, P, and O atoms (Figure 1), i.e. the (−α, −ζ) conformer of the R_p stereoisomer has the same energy as the (α, ζ) conformer of the corresponding S_p stereoisomer and vice versa. [h] Not a stationary point. [i] Saddle point of the second order.

independent dinucleotides form a duplex with the Watson−Crick base pairing. The (α, ζ) angles present in the crystal structure are equal to (−63°, −77°) and (−66°, −70°) for the first and second nonequivalent phosphonate linkages. On the other hand, the g⁻g conformation was observed in the crystal structure of the methylphosphonate (S_p)-containing d(Ap(CH_3)T) dinucleotide.[62] Here, however, dinucleotides do not form a duplex, but they are interconnected by the Hoogsteen-type base pairing.

(62) Chacko, K. K.; Lindner, K.; Saenger, W.; Miller, P. S. *Nucleic Acids Res.* **1983**, *11*, 2801.

The TS1 structure of DMPn is energetically and geometrically similar to the corresponding transition structure of DMP^-. However, the TS1 barrier can be circumvented in DMPn via the cis conformers denoted as TS5 (Figure 4). The pathway proceeds between these stationary points in the flat g^-g region mentioned above. Interestingly, although the free energy profiles for the S_p and R_p isomers are identical, the geometries involved are quite different from each other. Thus, in the S_p stereoisomer, the g^-g^- to gg transition is initiated by the rotation around the PO_3' bond. In contrast, in the R_p stereoisomer, the PO_5' bond must be rotated first because the inverted sequence of rotations results in an increase in the activation barrier by 1.5 kcal/mol. To base the explanation of the observed differences in the feasibility of the B-to-Z DNA transition in DNA containing different stereoisomers of DMPn[4] upon this stereoelectronic effect, one would have to assume that the 180° base-pair flip that occurs during the B−Z transition[63,64] places restrictions on the order in which α and ζ angles can be rotated from their equilibrium g^-g^- values. The viability of this mechanism cannot be evaluated without further calculations involving larger DNA fragments.

Alternatively, the observed inability of B-DNA containing the S_p phosphonate linkage to undergo the transition to the Z conformation[4] may involve differences in relative stabilities of such conformers of the S_p and R_p stereoisomers of DMPn that are structurally compatible with the left-handed DNA helix. Here, the relative energies of the R_p and S_p gg conformers of DMPn are identical. The LD solvation model indicates that these conformers should be more stable than the t^-g conformer, which also occurs frequently in Z-DNA, but the PCM model favors the reversed order of stability. For the t^-g (tg) conformer, the S_p stereoisomer was calculated to be more stable than the R_p stereoisomer. More specifically, the LD calculations predict that the S_p tg conformer is more stable by 2.4 kcal/mol than the R_p tg one, whereas the PCM calculations, which provide consistently lower solvation contributions, result in the free energy difference as large as 5 kcal/mol. Thus, the PCM solvation model favors strongly the left-handed S_p stereoisomer of the DNA phosphonate linkage over the linkage involving the left-handed R_p stereoisomer. This prediction is clearly in disagreement with the experimentally observed behavior. On the other hand, the LD calculations show no intrinsic conformational preferences for either stereoisomer. For this reason, and also because the PCM solvation energies vary within an unphysically small range upon the changes in the dipole moment of DMPn (Table 2S, see also Methods), the LD model represents our method of choice in this study. Consequently, only LD results are considered in Table 2, Figure 4, and in the subsequent text.

In summary, the stereoelectronic effects in aqueous solution calculated for DMPn seem to be too small to explain the different conformation preferences of DNA containing the S_p and R_p stereoisomers of the neutral dimethyl phosphonate linkage. In addition, we predict only negligible differences between the equilibrium conformational properties of DMPn and DMP^-. Therefore, the experimentally observed effects of the replacement of the ionic phosphate group in DNA by neutral methylphosphonate are likely to originate from the interactions between various DNA constituents on the level of the DNA secondary structure, as suggested by Callahan et al.[4] and Strauss and Maher.[9]

3.2.4. Dimethyl Phosphorothioate ($DMPTh^-$). Another useful experimental approach to determine the role played by the phosphate group in the B−Z DNA transition involves the stereospecific replacement of one of the ionic oxygens by a sulfur atom. Such a sulfur substitution retains the negative charge on the phosphate unit, but the longer PS bond and a larger size of the sulfur atom can have similar sterical effects on the B−Z transition as the $-CH_3$ group in DMPn. Indeed, akin to neutral phosphonates, phosphorothioates were found to induce significant changes in the thermodynamics and/or kinetics of the B−Z DNA conformational transitions.[5,6] Here, however, a large sequence dependence of the ability of phosphorothioate-containing DNA to undergo the B−Z transition, as well as the crystal structure of the R_p d(Gp(S)CpGp(S)CpGp(S)C) deoxyoligomer[65] implied only a minor role of the intrinsic conformational flexibility of the phosphorothioate linkage. Unfortunately, the experimental data for DNA backbones containing the DMPn and DMPTh groups cannot be directly compared since the relevant experiments involved oligomers that differed in length and the substitution pattern.

The calculated free energy barriers for conformational transitions in $DMPTh^-$ are presented in Table 2 and Figure 4. These data show that there are two low-energy pathways which can connect the g^-g^- and gg conformers. Both pathways are similar to the low-energy pathways calculated for DMP^-, in particular because their activation barriers correspond to TS1 structures. A further reaction-coordinate branching, analogous to that described for DMP^-, is energetically feasible (Table 2). However, for the sake of simplicity, this branching was not depicted in Figure 4. Overall, small calculated differences in the involved activation barriers indicate that any of several pathways for the B-to-Z transition can be selected by the specific DNA environment.

In addition, our calculations show that the most stable structure of $DMPTh^-$ in aqueous solution should correspond to its gt conformer. This finding is in excellent agreement with the X-ray crystal structures of diethyl phosphorothioate[53] and uridine thiophosphate methyl ester (R_p).[66] Interestingly, the gt conformation for the OPOC angles can be alternatively viewed as the gauche−gauche conformation for the SPOC angles. As pointed out by Schwalbe et al.,[53] the gauche arrangement of the PS bond to both OC bonds is not obvious a priori in view of the bulk of the sulfur atom. The experimental values of the SPOC angles amount to (48°; 39°), (66°; 39°), and (47°; 33°) for diethyl phosphorothioate[53] and for two nonequivalent structures of uridine thiophosphate methyl ester,[66] while our calculated SPOC torsional angles are 73.1° and 50.3°. The small difference between the theoretical and X-ray SPOC angles can be attributed to the intermolecular interactions in the crystals and to the fact that the calculated structure was obtained by the geometry optimization in the gas phase. Because solvation effects tend to stabilize the conformers with the methyl groups oriented toward the sulfur atom, geometry optimization in solution would most probably result in somewhat smaller SPOC angles and improve further the agreement with X-ray data.

Conclusions

In this work, we carried out the conformational analysis of the dimethyl phosphate anion, dimethyl phosphorothioate anion, dimethyl methylphosphonate, and methyl ethylphosphonate anion in the gas phase and in aqueous solution. Our calculations indicated the following:

(63) Olson, W. K. In *Biomolecular Stereodynamics*; Sarma, R. H., Ed.; Adenine Press: New York, 1981; Vol. 1; p 327.
(64) Sarma, M. H.; Gupta, G.; Dhingra, M. M.; Sarma, R. H. *J. Biomol. Struct. Dyn.* **1983**, *1*, 59.
(65) Cruse, W. B. T.; Salisbury, S. A.; Brown, T.; Cosstick, R.; Eckstein, F.; Kennard, O. *J. Mol. Biol.* **1986**, *192*, 891.
(66) Saenger, W.; Suck, D.; Eckstein, F. *Eur. J. Biochem.* **1974**, *46*, 559.

1. Aqueous solvation effects play a significant role for conformational stability and kinetics of conformational transitions of these esters. For example, the gauche−gauche conformer of the neutral methylphosphonate, which has a relative gas-phase free energy 2.3 kcal/mol above the trans−gauche conformers, is predicted to be the most stable structure in aqueous solution. Overall, the solvation effects on the relative stability of different conformers were found to be smaller for ionic compounds than for the neutral phosphonate.

2. The replacement of either O3′ or O5′ oxygen in the phosphodiester bonds increases the local flexibility of the resulting DNA linkage. This property could be utilized, for example, in the design of highly flexible ribozymes or antisense oligonucleotides.

3. The torsional angles of the gg conformers of dimethyl phosphate anion and of both stereoisomers of the neutral methyl phosphonate are quite similar. Consequently, stereospecific replacement of the phosphate group in nucleic acids by neutral methylphosphonate can be used to selectively probe the structural effects of intermolecular interactions involving individual ionic phosphate oxygens. On the other hand, we found significant differences in the geometries of transition states for conformational transitions in these compounds. Therefore, stereoelectronic effects should be considered in structural interpretations of kinetic studies of DNA molecules containing neutral phosphonate linkages.

4. The replacement of an ionic phosphate oxygen by sulfur leads to the enhanced stabilization of the gt conformer, whereas the free energy profile for the transition from the right- to the left-handed conformer of dimethyl phosphorothioate retains features similar to those of the parent compound.

Acknowledgment. This work was supported by the Grant Agency of the Czech Republic and by the UC-Berkeley Tobacco-Related Disease Research Grant (4RT-0002). We also thank Dr. T. Glennon for language corrections and helpful comments.

Supporting Information Available: Numbering and HF/6-31G* and MP2/6-31+G** geometries of the gg conformers of the title compounds; conformational dependence of the ESP PCM/HF/6-31G* atomic charges, PCM solvation free energies, and dipole moments of DMP^-, DMPn, and $DMPTh^-$; electrostatic, van der Waals, hydrophobic, solute polarization, and electron correlation contributions to the LD hydration free energies of title compounds; and electrostatic-potential-derived atomic charges of the gg conformers of title compounds calculated at the HF/6-31G*, MP2/6-31+G**, and PCM/HF/6-31G* levels (6 pages, print (PDF). See any current masthead page for ordering information and web access instructions.

JA9710823